Materials Science Forum Vols. 600-603 (2009) pp 279-284
online at http://www.scientific.net

EPR Identification of Defects and Impurities in SiC: To be decisive

J. Isoya[1,a], T. Umeda[1], N. Mizuochi[1], N.T. Son[2], E. Janzén[2] and T. Ohshima[3]

[1)]University of Tsukuba,Tsukuba 305-8550, Japan, [2)]Department of Physics, Chemistry and Biology, Linköping University, SE-581 83 Linköping, Sweden
[3)]Japan Atomic Energy Agency, Takasaki 370-1292, Japan
[a]isoya@slis.tsukuba.ac.jp

Keywords: SiC, EPR, ENDOR, defects, impurities

Abstract. In EPR (electron paramagnetic resonance) identification of point defects, hyperfine (HF) interaction is decisive information not only for chemical identity but also for the local geometry and the electronic state. In some intrinsic defects in SiC, the wave function of the unpaired electron extends quite unevenly among major atoms comprising the defects. In such a case, the determination of the number of equivalent atoms and the chemical identity (Si or C) of those atoms even with weak HF splitting are useful to compare with HF parameters obtained theoretically. For vacancy-related defects of relatively deep levels, the sum of the spin densities on the nearest-neighbor shell is found to be 60-68%.

Introduction. Among new semiconductor materials with which electronic devices having performances and functions not feasible with silicon are exploited, SiC is promising for high-power, high-temperature, and radiation-tolerant devices. Physical properties of SiC crystals are strongly affected by point defects even with a low concentration. While most of point defects spoil the device properties, doping of shallow donors and acceptors is essential in fabrication of devices and moreover, semi-insulating (SI) substrates are attained by utilizing intrinsic defects. To solve problems such as obtaining high-quality substrates and epilayers and improving efficiency of ion implantation doping, understanding of behaviors of point-defects is critically important. In structure determination of point defects in silicon, the most successful technique proved to be EPR. In SiC of a complexity coming from compound semiconductors, EPR identification of point defects is often not straightforward, however, is likely to be equally successful as in silicon, with careful measurements and with the benefit of theoretical HF parameters which are nowadays provided by *first principles* calculations.

Keys to EPR identification. In EPR spectra of point defects in SiC, several sets (i=1,2, ··) of ^{29}Si and/or ^{13}C hyperfine (HF) lines are expected to appear as satellite lines of the strong primary lines. The angular dependences of the line positions of i-th hyperfine satellite lines are described by the spin-Hamiltonian

$$\mathcal{H} = [\beta_e \mathbf{S}\cdot\mathbf{g}\cdot\mathbf{B} + \mathbf{S}\cdot\mathbf{D}\cdot\mathbf{S} + + \mathbf{S}\cdot\mathbf{A}_{imp}\cdot\mathbf{I}_{imp}] + \mathbf{S}\cdot\mathbf{A}_i\cdot\mathbf{I}_i - g_n\beta_n\mathbf{I}_i\cdot\mathbf{B}. \quad (1)$$

The line positions of the primary lines are determined by **g**, by **D** in the case of $S\geq 1$, and by $\mathbf{A}_{imp}$ in the case of impurities with magnetic nuclei such as ^{14}N (I=1, 99.6%) and ^{31}P (I=1/2, 100%). The low abundances of the isotopes with non-zero nuclear spin (^{29}Si, I=1/2, 4.7%, ^{13}C, I=1/2, 1.1%), limiting severely the intensity of the HF satellite lines, bring a good resolution with the narrow line width (ΔB_{pp}~0.03mT) for both primary and satellite lines. For impurities, while chemical identities are obtained by HF of the primary lines ($\mathbf{A}_{imp}$), the ^{29}Si/^{13}C satellite lines are useful in determining the sublattice (Si or C) occupied [1, 2]. In the case of intrinsic defects, the primary lines are useful in

distinguishing EPR spectra from different defects. Until microscopic structure model is established, EPR spectra are referred tentatively by using labels (n=1,2,3, ⋯) like SIn, EIn, HEIn for those which were found in SI substrates, in electron-irradiated samples, and after electron irradiation at high temperatures, respectively, and like Pn, Tn, ·· by the initials indicating the research group. For building up the structure model of intrinsic defects, HF satellite lines are most informative. From the HF tensor $\mathbf{A}_i$ determined from the angular dependence of the ^{29}Si/^{13}C HF lines of the i-th Si/C atom comprising a point defect, the orbital parameters of the i-th atom such as the spin density η_i^2, the sp hybrid ratio β_i^2/α_i^2, and the direction of the p_i-orbital with respect to the crystal axes are obtained. Here, we use a LCAO description for the wave function of the unpaired electron

$$\Psi = \Sigma_i \, \eta_i (\alpha_i \varphi_{si} + \beta_i \varphi_{pi}), \qquad (2)$$

where $\alpha_i^2+\beta_i^2=1$ and φ_{si}, φ_{pi} are $2s$, $2p$ for i-th carbon or $3s$, $3p$ for i-th silicon. The tensor $\mathbf{A}_i$ is uniaxial with the principal values $A_{//}$ ($A_{iso}+2b$) and $A_{\perp}$ ($A_{iso}-b$) or is nearly uniaxial. From the isotropic part A_{iso} and the anisotropic part b, the orbital parameters are estimated ($\eta_i^2\alpha_i^2=A_{iso}/A_0$, $\eta_i^2\beta_i^2=b/b_0$), where we use (134.77mT, 3.83mT) and (-163.93mT, -4.075mT) for (A_0, b_0) of ^{13}C and that of ^{29}Si, respectively [3]. For atoms with a small spin density, dipolar field from the spin density on other atom(s) might be also taken into account as a source of the anisotropic part of HF.

In structure determination of an intrinsic defect, obtaining the orbital parameters from all major atoms comprising the defect such as four nearest-neighbors in a vacancy and six nearest-neighbors in a divacancy is crucially important. As in the cases of divacancy $[V_{Si}V_C]^0$, the unpaired electron might be localized mostly on a part of the major component atoms [4]. For some of the major-component atoms which exhibit weak HF splitting, although only the number of equivalent atoms and $\eta_i^2\alpha_i^2$ are obtained, these information is still important to compare with the HF parameters estimated from theoretical studies. To extract weak HF interaction or small anisotropy of HF interaction which is hidden underneath the line broadening of conventional cw(continuous wave)-EPR, we apply pulsed ENDOR (electron nuclear double resonance) and ESEEM (electron spin echo envelope modulation) [1, 2,5]. These methods obtaining the ENDOR frequencies ($\nu_N=|M_S\cdot A_{eff}/2-g_N\beta_N B|$) are also useful to identify the nucleus (^{29}Si or ^{13}C) giving rise to the resolved HF satellite lines [6]. After identifying the nucleus (^{29}Si or ^{13}C), the number of equivalent atoms is determined for each of HF satellite lines from the intensity relative to the primary line.

Spin multiplicity. The determination of the spin multiplicity (S) is important to determine the charge state. For $S\geq1$, zero-field splitting (**D**) splits the primary lines into $2S$ lines. However, for V_{Si}^- with the absence of the zero-field splitting, S=3/2 was determined by ENDOR [7]. The spin multiplicity (S=3/2) of T_{V2a} was determined by nutation method of pulsed technique [8] and by pulsed ENDOR [9]. Thus, T_{V2a} belongs to a family of V_{Si}^-.

Separation of overlapping spectra. We use both cw-EPR and pulsed EPR. To enhance spectral resolution, one way is to increase the difference in the field positions of the primary lines with different g values by utilizing high frequencies such as Q-band (35GHz) and W-band (240GHz).

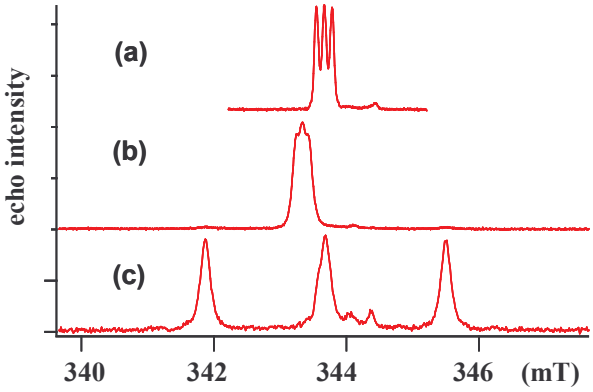

Fig.1 Echo-detected EPR of (a)3C-SiC:N, 20K (b)4H-SiC:N(h), 10K and (c) 4H-SiC:N(k), 40K (B//[0001] for 4H-SiC). Resolution compatible to that of cw-EPR is obtainable. Moreover, by utilizing the difference in T_1, N(h) and N(k) spectra are separately observed.

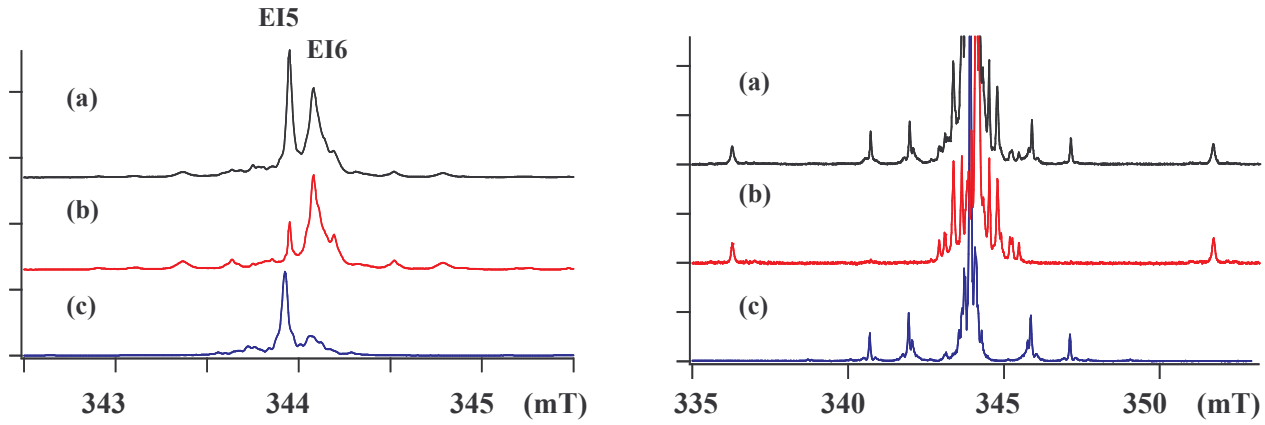

Fig. 2 Separation of EI5/EI6 spectra by echo-detected EPR. Primary lines (left panel) and ^{29}Si HF lines (right panel) are shown, respectively. (a) 10K, τ=1μs, repetition delay (r.d.)=8ms, (b) 10K, τ=20μs, r.d.=8ms, (c) 5K, τ=1.2μs, r.d.=1ms.

However, sometimes, HF lines overlap with primary lines of other centers in the high frequency measurements. For such a case, X-band frequency (10GHz) gives better angular-dependence data. In our X-band pulsed EPR measurements, a field-swept spectrum (echo-detected EPR) is obtained by measuring the intensity of 2-pulse echo (90°–τ–180°–τ–echo) as a function of the magnetic field. In echo-detected EPR, while using a strong microwave pulse (~1mT), the resolution similar to cw-EPR is obtainable by using a selective detection (See, Figs.1, 2). In 4*H*-SiC, $V_C(k)^+$ undergoes thermally activated reorientation among symmetry-lowered configurations of C_{1h} symmetry [5,6]. In the low temperature spectrum of $V_C(k)^+$, both phase memory time T_M (the time constant of 2-pulse echo decay) and the spin-lattice relaxation time T_1 (the time required for M_z to recover to thermal equilibrium value) is much shorter than those of $V_C(h)^+$. Fig. 2a shows the standard spectra using the echo-detected EPR. With using a large τ, echo-detected EPR spectrum with $V_C(k)^+$ suppressed considerably is obtained (Fig.2b). With using a short delay in repeating the pulse sequence in accumulation, echo-detected EPR spectrum with $V_C(h)^+$ suppressed is obtained (Fig.2c).

Production and thermal behavior. The production and thermal behaviors useful in identification of defects are monitored by strong primary lines by which defects are distinguished. To track the angular dependence of the ^{29}Si/^{13}C HF lines which does lead to decisive structure determination, it is desirable to produce the intrinsic defect of interest selectively at sufficient concentration. For intrinsic defects, we took a sort of defect engineering approach by using various combinations of the temperature (40-800°C) of 3MeV electron irradiation, the total dose (1×10^{17}-1×10^{19} e/cm^2), the heat-treatment (400-1200°C) after irradiation, and 4*H*-SiC samples (3×10×1.5mm) of both *n*- and *p*-type of different dopant concentrations.

Symmetry. In 4*H*-SiC, point defects preserving the C_{3v} symmetry of the lattice has one magnetically distinguishable site with both **g** and **D** ($S\geq1$) having axial symmetry. The line positions of primary lines depend on the angle between **B** and the c-axis. When symmetry is lowered to C_{1h}, the presence of symmetry-related sites which have same structure except different orientations splits the primary lines upon rotating from the *c*-axis. Utilizing the orientational degeneracy of symmetry-related sites, EPR parameters for C_{1h} symmetry are obtained by a rotation of the crystal about one axis ([11-20] or [1-100]), as in the case of C_{3v} symmetry. In $V_{Si}^-$and T_{v2a} which have the C_{3V} symmetry, among the four nearest-neighbor carbons, one located along the *c*-axis has C_{3v} symmetry while the ^{13}C hyperfine lines of basal carbon atoms split into four lines (1:1:2:2) in the rotation around the [11-20] axis (There are two orientations of tetrahedron of four carbon atoms) [8,10]. From the pattern of the angular dependence and the number of equivalent sites at special directions, the symmetry is determined.

Hexagonal(*h*) and cubic(*k*) sites. SiC is unique in abundant polytypes. For intrinsic defects, we mostly work on 4*H*-SiC, in which both silicon and carbon atoms have two inequivalent lattice sites, hexagonal (*h*) and quasi-cubic (*k*) sites. It is desirable to list up a set of EPR spectra originating from the two inequivalent sites. Defects corresponding to the two different sites are expected to have different configurations which are distinguishable by EPR, however, to have a similar production and annealing behaviors. Observation of four configurations (*hh*, *kk*, *hk*, *kh*) is a basis of both assignments, P6(C_{3v}, S=1) / P7(C_{1h}, S=1) to divacancy $[V_{Si}V_C]^0$ [4] and HEI9 / HEI10 to positively charged carbon antisite-vacancy pair $C_{Si}V_C^+$ [11]. With the development of *first principles* calculations, HF interactions are used to examine a defect model. Calculated HF interactions are helpful to assign the site (*h* or *k*) [1]. A remarkable difference in the Jahn-Teller distortion between $V_C^+(h)$ and $V_C^+(k)$ was first pointed out by theoretical studies [12,13] and EI6/EI5 spectra correspond to $V_C^+(h)/V_C^+(k)$ [5,6].

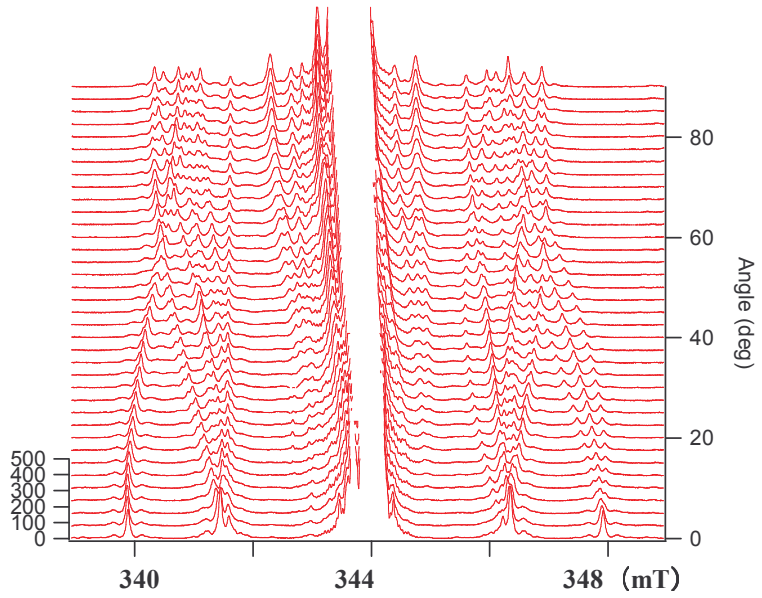

Fig.3. Angular dependence of ^{29}Si hyperfine lines of $V_C^+(k)$ at 5K by echo-detected EPR (**B**⊥[[1-100]). Note that disturbing signals from other centers are considerably suppressed.

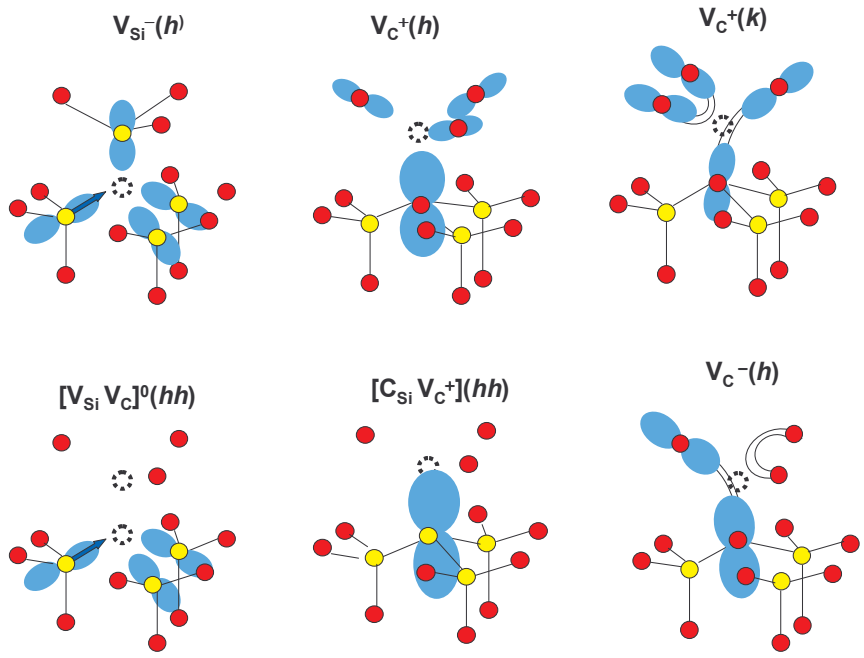

Fig.4 Schematic view of the distribution of spin densities among the nearest-neighbors of vacancy-related defects in 4*H*-SiC

Table I. Spin densities ($\eta^2_{\text{shell-I}}$: sum of η_i^2 of nearest-neighbors), *sp*-hybrid ratio (β_i^2/α_i^2), and angle (θ_i) between the direction of p_i-orbital and the c-axis determined by EPR for vacancy-related centers in 4*H*-SiC

EPR center and defect model	symmetry of center	atoms	η_i^2 (%)	$\eta^2_{\text{shell-I}}$ (%)	β_i^2/α_i^2	θ_i	Ref.
EI6 $V_C^+(h)$	150K C_{3v}	$Si_{I(1)}$ $Si_{I(2,3,4)}$	33.4 9.3	61.3	5.3 5.5	0° 102.6°	[5]
	5 K C_{3v}	$Si_{I(1)}$ $Si_{I(2,3,4)}$	47.3 6.9	68.0	5.3 5.9	0° 97.7°	[6]
EI5 $V_C^+(k)$	150K C_{3v}	$Si_{I(1)}$ $Si_{I(2,3,4)}$	19.6 15.1	64.9	5.3 5.0	0° 109.2°	[5]
	5 K C_{1h}	$Si_{I(1)}$ $Si_{I(2)}$ $Si_{I(3,4)}$	19.9 14.7 16.5	67.6	5.4 5.4 5.1	7.7° 121.5° 103.2°	[6]
P6b $[V_{Si}V_C]^0(hh)$	77 K C_{3v}	$C_{I(2,3,4)}$ $Si_{I(2,3,4)}$ $Si_{II(1,2,3)}$ $Si_{II(4\text{-}9)}$	20.0 0.07 0.26 0.20	60.2	9.7	117°	[4]
HEI1 $V_C^-(h)$	60K C_{1h}	$Si_{I(1)}$ $Si_{I(2)}$	24.1 36.6	60.7	3.6 3.6	7° 101°	[14]
V_{Si}^-(I) $V_{Si}^-(h)$ V_{Si}^- (II) $V_{Si}^-(k)$	295 K C_{3v}	$C_{I(1)}$ $C_{I(2,3,4)}$ $C_{I(1)}$ $C_{I(2,3,4)}$	15.9 15.9 16.1 16.2	63.6 64.7	11.3 11.2 12.7 11.9	0° 110.0° 0° 109.2°	[10]
T_{V2a} distorted V_{Si}^-	160K C_{3v}	$C_{I(1)}$ $C_{I(2,3,4)}$	15.4 15.6	62.2	10.7 12.2	0° 107.5°	[8]
HEI9a $C_{Si}V_C^+(hh)$	295 K C_{3v}	C_{Si}	55.2	—	16.4	0°	[11]
SI5 $C_{Si}V_C^-$	30K C_{1h}	$Si_{1,2}$	30.3	—	3.5	111°	[15]

In V_{Si}^- (S=3/2), the isotropic **g**, the isotropic ^{29}Si HF interaction of next-nearest-neighbors and the absence of the zero field splitting were ascribed to local tetrahedral arrangement. The angular dependence of the ^{13}C HF lines of the nearest-neighbors revealed the C_{3v} symmetry and resolved two spectra V_{Si}^-(I) and V_{Si}^-(II) arising from the inequivalent lattice sites [10]. The difference in the spin density between the axial and basal carbon atoms and the deviation of the 2*p*-orbital direction of the basal carbon from the tetrahedral angle were detected. Assignment, V_{Si}^-(I)/V_{Si}^-(II) to $V_{Si}^-(h)$/$V_{Si}^-(k)$, is based on the signal intensity ratio of the corresponding centers in 6*H*-SiC.

Comparison among vacancy-related defects.

The orbital parameters obtained for vacancy-related centers in 4*H*-SiC are listed in Table I (See Fig.4). We note that the sum of the spin densities of the nearest-neighbors $\eta^2_{\text{shell–I}}$ is 60–68%, regardless of vacancy site (Si/C or *h*/*k*). The *sp* hybrid ratio (β_i^2/α_i^2) varies from 3.5 to 16.4. The larger value of β_i^2/α_i^2 is likely to be caused by dominant breathing relaxation. It should be noted that ($\eta^2_{\text{shell–I}}$, β_i^2/α_i^2) are estimated to be (83%, 6.9), (82%, 9.0), (55%, 2.5) and (58%, 5.5), respectively, for V^-(T_d, S=3/2), $[VV]^0$ (C_{2h}, S=1) in diamond [16, 17] and V^- (C_{2v}, S=1/2), V^+ (D_{2d}, S=1/2) in silicon [18, 19].

Acknowledgements.
Here we review our works from the experimentalist side. Our identification of point defects has been achieved with collaboration with theoretical groups, A. Gali (Budapest University of Technology and Economics) and M. Bockstedte (Universität Erlangen-Nürunberg).

References

[1] N. T. Son, A. Henry, J. Isoya, M. Katagiri, T. Umeda, A. Gali, and E. Janzén, Phys. Rev. B Vol. 73 (2006), 075201.

[2] N. T. Son, E. Janzén, J. Isoya, and S. Yamasaki, Phys. Rev. B Vol. 70 (2004), p.193207.

[3]J. A. Weil, J. R. Bolton, J. E. Wertz: *Electron Paramagnetic Resonance* (John Wiley & Sons, NY 1994).

[4] N. T. Son, P. Carlsson, J. ul Hassan, E. Janzén, T. Umeda, J. Isoya, A. Gali, M. Bockstedte, N. Morishita, T. Ohshima, and H. Itoh, Phys. Rev. Lett. Vol. 96 (2006), p.055501.

[5] T. Umeda, J. Isoya, N. Morishita, T. Ohshima, and T. Kamiya, Phys. Rev. B Vol. 69 (2004), p.121201(R).

[6] T. Umeda, J. Isoya, N. Morishita, T. Ohshima, T. Kamiya, A. Gali, P. Deák, N. T. Son, and E. Janzén, Phys. Rev. B Vol. 70 (2004), p.235212.

[7] T. Wimbauer, B. K. Meyer, A. Hofstaetter, A. Scharmann. and H. Overhof, Phys. Rev. B Vol. 56 (1997), p.7384.

[8] N. Mizuochi, S. Yamasaki, H. Takizawa, N. Morishita, T. Ohshima, H. Itoh, and J. Isoya, Phys. Rev. B Vol. 66 (2002), p.235202

[9] N. Mizuochi, S. Yamasaki, H. Takizawa, N. Morishita, T. Ohshima, H. Itoh, T. Umeda, and J. Isoya, Phys. Rev. B Vol. 72 (2005), p.235208.

[10] N. Mizuochi, S. Yamasaki, H. Takizawa, N. Morishita, T. Ohshima, H. Itoh, and J. Isoya, Phys. Rev. B Vol.68 (2003), p.165206.

[11] T. Umeda, J. Isoya, T. Ohshima, N. Morishita, H. Itoh, and A. Gali, Phys. Rev. B Vol. 75 (2007), p.245202.

[12] M. Bockstedte, M. Heid, and O. Pankratov, Phys. Rev. B Vol. 67 (2003), p.193102.

[13] A. Gali, P. Deák, N. T. Son, and E. Janzén, Mater. Sci. Forum Vol. 433-436 (2003), p.511.

[14] T. Umeda, Y. Ishitsuka, J. Isoya, N. T. Son, E. Janzén, N. Morishita, T. Ohshima, H. Itoh, Phys. Rev. B Vol. 71 (2005), p.193202.

[15] T. Umeda, N. T. Son, J. Isoya, E. Janzén, T. Ohshima, N. Morishita, H. Itoh, A. Gali, and M. Bockstedte, Phys. Rev. Lett. Vol. 96 (2006), p.145501.

[16] J. Isoya, H. Kanda, Y. Uchida, S. C. Lawson, S. Yamasaki, H. Itoh, and Y. Morita, Phys. Rev. B Vol. 45 (1992), p.1436.

[17] D. J. Twitchen, M. E. Newton, J. M. Baker, T. R. Anthony, and W. F. Banholzer, Phys. Rev. B Vol.59 (1999), p.12900.

[18] M. Sprenger, S. H. Muller, E. G. Sieverts, and C. A. J. Ammerlaan, Phys. Rev. B Vol.35 (1987), p.1566.

[19]G. D. Watkins, J. Phys. Soc. Jpn. Vol.18, Suppl. II (1963), p.22.